Supplemental Materials

Molecular Biology of the Cell

Steinfeld *et al*.

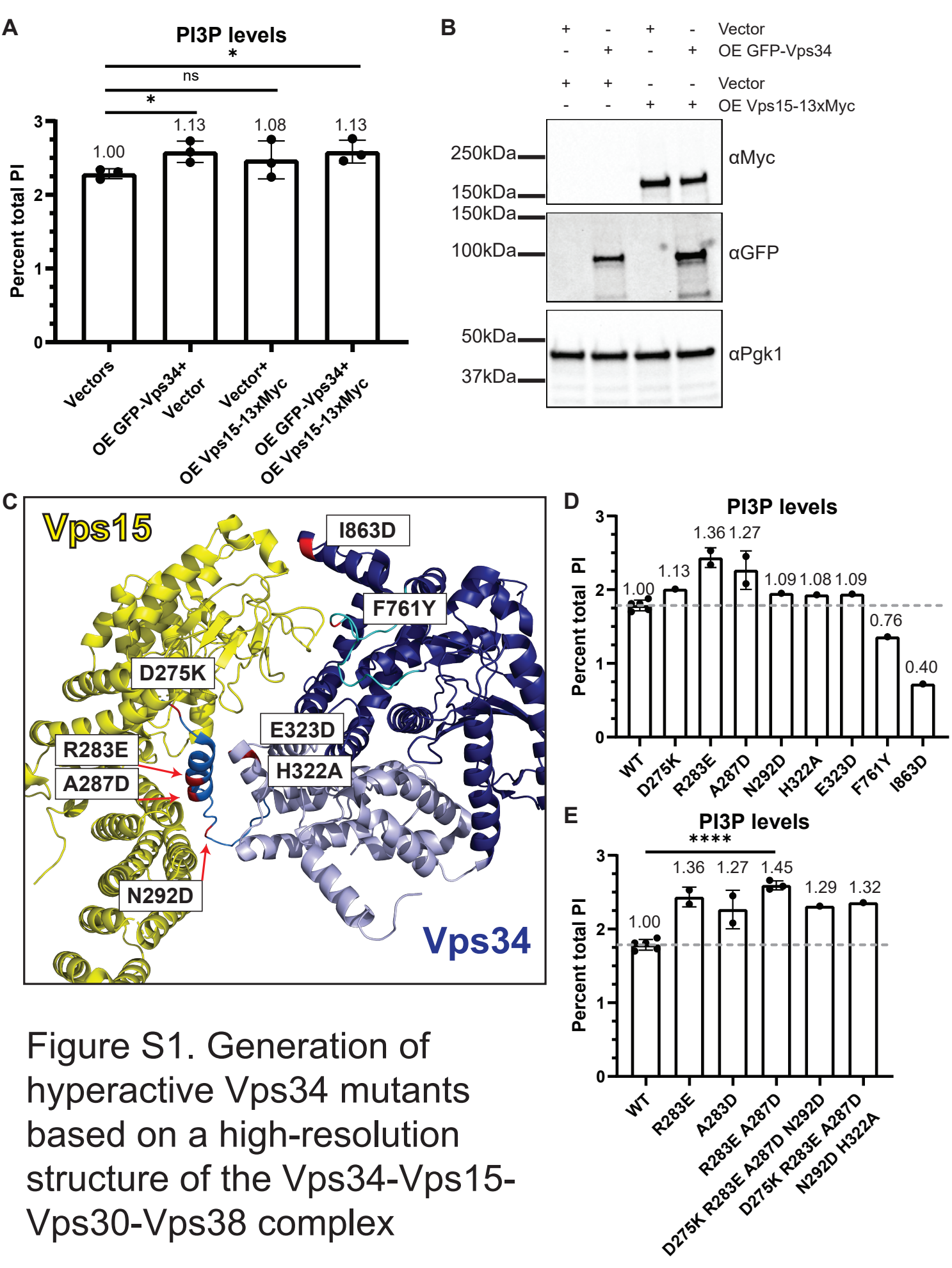

Figure S1. Generation of hyperactive Vps34 mutants based on a high-resolution structure of the Vps34-Vps15-Vps30-Vps38 complex

Figure S1. Generation of hyperactive Vps34 mutants based on a high-resolution structure of the Vps34-Vps15-Vps30-Vps38 complex. (A and B) Overexpression of GFP-Vps34 and Vps15-13xMyc results in a modest 13% increase in PI3P levels. Wild-type yeast cells were transformed with pRS426-GFP-Vps34, pRS425-Vps15-13xMyc, or both plasmids together. PPI lipid levels were measured. In parallel, GFP-Vps34 and Vps15-13xMyc protein levels were analyzed via western blot to measure overexpression. Vps15-13xMyc was detected using anti-Myc antibody. GFP-Vps34 was detected with anti-GFP antibody. Pgk1 was used as a loading control. Representative of n=3. PPI lipid levels were measured by metabolically labeling cells with myo-^{3}H-inositol for 16 h, harvesting cells, and separating PPI lipid head groups by anion exchange and HPLC. n=3. Error bars indicate standard deviation. Unpaired t-test. ns=p>.05, *=p<.05. (C) Based on the crystal structure of the PI 3-kinase complex and the hypothesis that altering the contact between Vps34 HELCAT (helical in light blue kinase in dark blue) and Vps15 (yellow) would activate Vps34, we tested eight point mutants (red) in Vps34 for elevated PI3P levels (Rostislavleva *et al.*, 2015; Stjepanovic *et al.*, 2017). D275K, R283E, A287D, and N292D are on an alpha-helix N-terminal to the helical domain of Vps34 (neutral blue), E323D and H322A are in the helical domain, F761Y is in the activation loop (cyan), and I863D is in the kinase domain. (D and E) Of the mutants predicted to disrupt the interaction between Vps34 HELCAT and Vps15, PI3P levels are most elevated by R283E and A287D (D). Combination of R283E with A287D further elevated PI3P levels (E). However, combining R283E A287D with additional mutations did not further elevated PI3P levels (E). *vps34Δ* cells were transformed with a wild-type or mutant pRS416-Vps34 plasmid. PPI lipid levels were measured by metabolically labeling cells with myo-^{3}H-inositol for 16 h, harvesting cells, and separating PPI lipid head groups by anion exchange and HPLC. n=5 for WT, n=2 for R283E and A287D, n=3 for R283E A287D, n=1 for the rest. WT, R283E, and A287D data points are the same in D and E. Error bars indicate standard deviation. Unpaired t-test. ****=p<.0001.

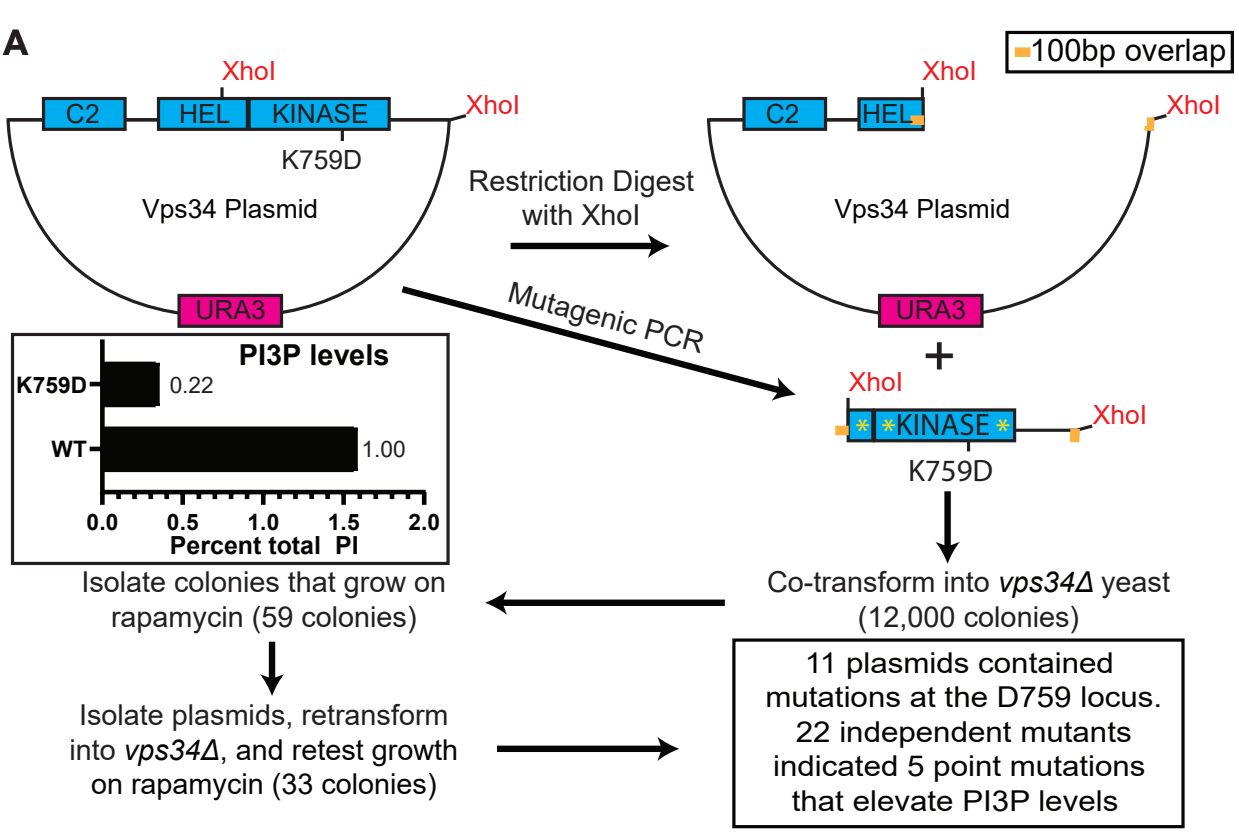

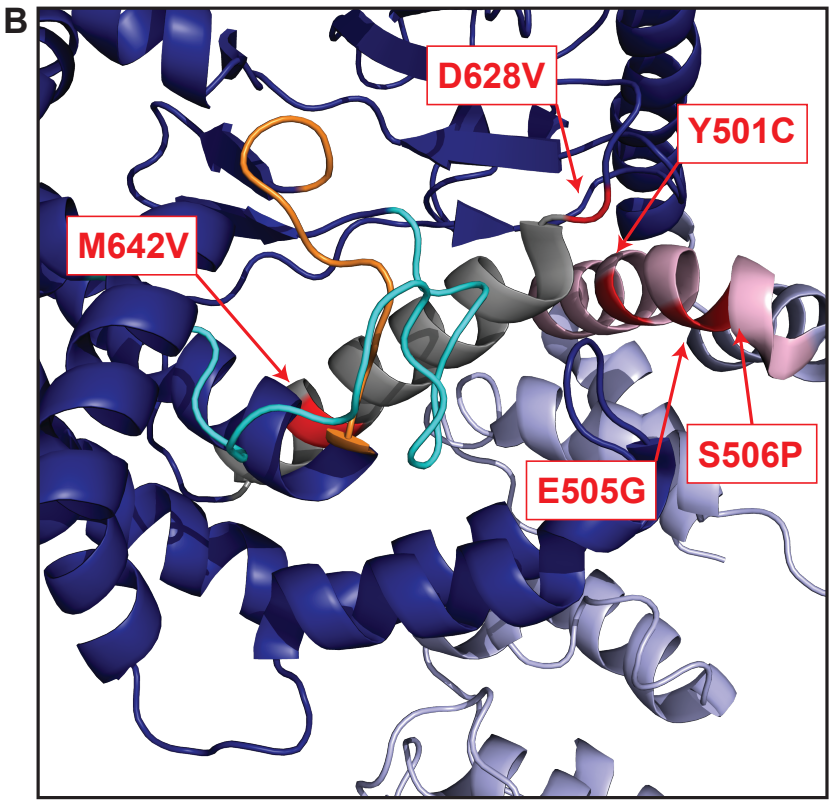

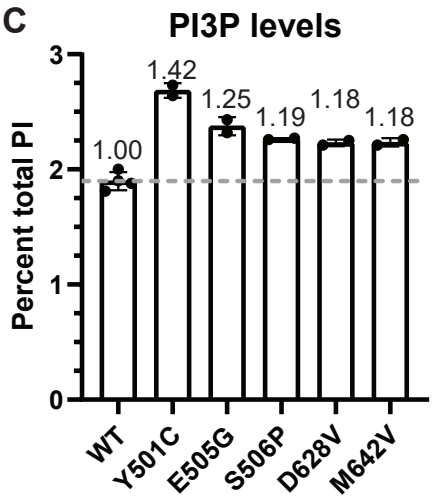

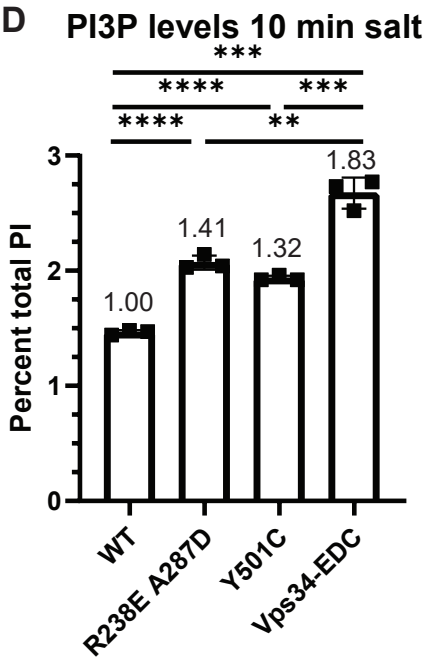

Figure S2. Generation of hyperactive Vps34 mutants via a mutant screen

Figure S2. Generation of hyperactive Vps34 mutants via a mutant screen. (A) A screen for hyperactive mutations in Vps34 was designed to identify mutants that rescued growth of a hypomorphic Vps34 allele, Vps34-K759D, a mutation in the activation loop of Vps34 that lowers PI3P levels to 22% of wild-type. *vps34Δ* cells were transformed with pRS416-Vps34 or pRS416-Vps34-K759D plasmids. PPI lipid levels were measured by metabolically labeling cells with myo-^{3}H-inositol for 16 h, harvesting cells, and separating PPI lipid head groups by anion exchange and HPLC. n=1. The C-terminal half of Vps34 was PCR amplified using mutagenic Taq DNA polymerase and a Vps34 plasmid was cut with restriction enzyme, XhoI, to remove the region of Vps34 that was mutated. The plasmid backbone and mutated PCR fragment were co-transformed into *vps34Δ* cells. Two days following co-transformation, colonies were replica plated to plates containing 10 nM rapamycin and grown at 33°C. Mutant Vps34 plasmids were isolated from colonies that rescued growth on rapamycin at 33°C and retransformed into *vps34Δ* cells to confirm rescued growth on rapamycin at 33°C. Sanger sequencing was used to identify the mutations present in isolated plasmids. 22 independent mutants revealed nine unique point mutations. Of those nine mutations, changes at five of them were found to elevate PI3P levels. (B) Crystal structure of the helical (light blue) and kinase (dark blue) domains of Vps34, indicating five residues identified in the hyperactive Vps34 mutant screen (red). M642V and D628V are at opposite ends of the alpha-C helix (gray) of the kinase domain, nearby the activation (cyan) and catalytic (orange) loops of Vps34. Y501C, E505G, and S506P face the alpha-C helix on the same side of an alpha helix in the helical domain of Vps34 (light pink). (C) Of the mutants identified in the Vps34 hyperactive mutant screen, PI3P levels are most elevated by Y501C. *vps34Δ* cells were transformed with a wild-type or mutant pRS416-Vps34 plasmid. PPI lipid levels were measured by metabolically labeling cells with myo-^{3}H-inositol for 16 h, harvesting cells, and separating PPI lipid head groups by anion exchange and HPLC. n=4 for WT, n=2 for the rest. Error bars indicate standard deviation. (D) The Vps34 mutants R283E A287D and Y501C elevate PI3P levels during hyperosmotic shock. Combining the mutants to generate Vps34-EDC further elevated PI3P during hyperosmotic shock. *vps34Δ* cells were transformed with a wild-type or mutant pRS416-Vps34 plasmid. PPI lipid levels were measured by metabolically labeling cells with myo-^{3}H-inositol for 16 h. Prior to harvest, indicated cultures were exposed to 10 min of hyperosmotic shock. PPI lipid head groups were separated by anion exchange and HPLC. Data are from the same samples as Figure 1D-F. n=3. Error bars indicate standard deviation. Unpaired t-test. **=p<.01, ***=p<.001, ****=p<.0001.

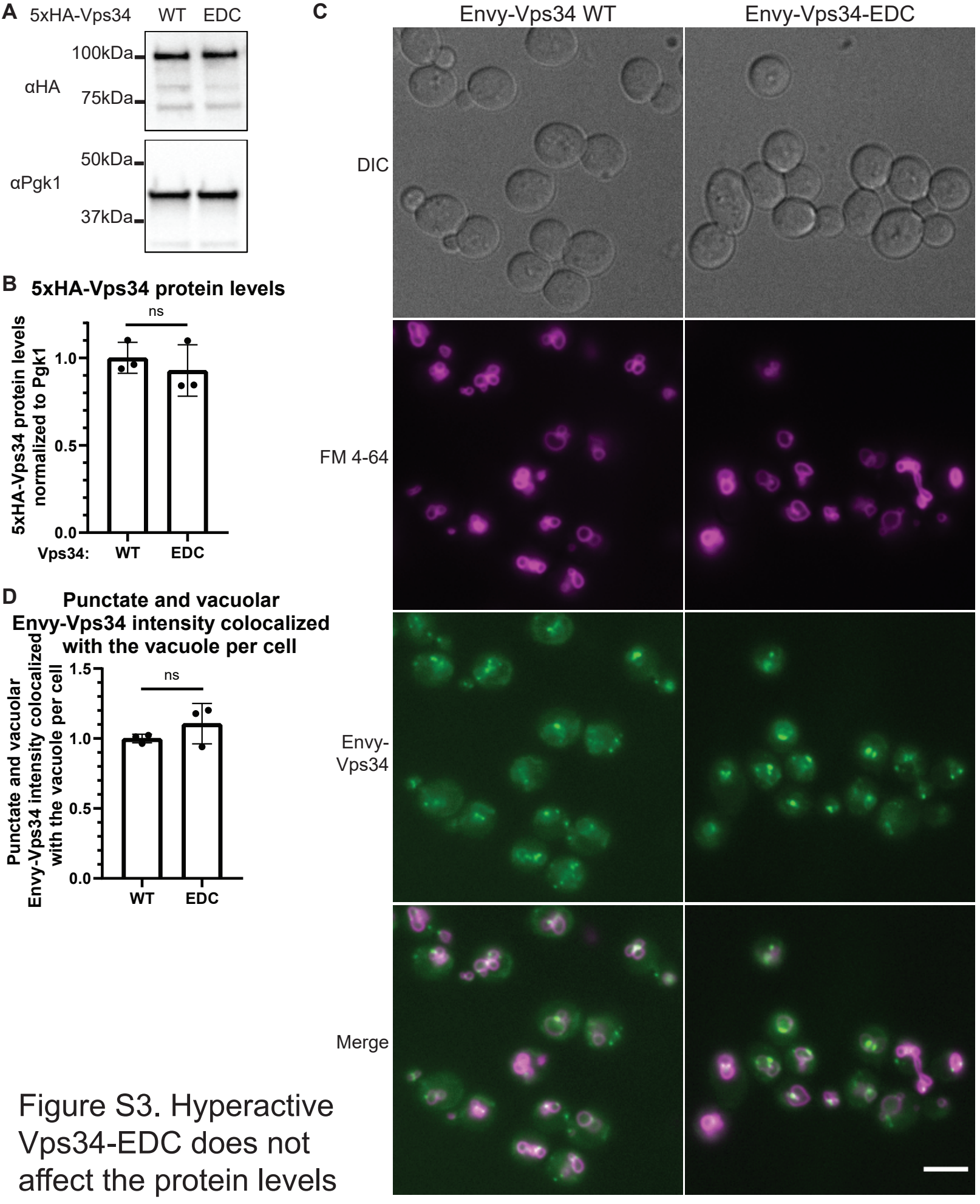

Figure S3. Hyperactive Vps34-EDC does not affect the protein levels or localization of Vps34

Figure S3. Hyperactive Vps34-EDC does not affect the protein levels or localization of Vps34. (A and B) Hyperactive Vps34-EDC does not change 5xHA-Vps34 protein levels. *vps34Δ* cells were transformed with pRS416-5xHA-Vps34 or pRS416-5xHA-Vps34-EDC. 5xHA-Vps34 protein levels were analyzed via western blot using anti-HA antibody. 5xHA-Vps34 levels were normalized to Pgk1. Levels were then normalized to wild-type. Representative of n=3. Error bars indicate standard deviation. Unpaired t-test. ns=p>.05. (C and D) Hyperactive Vps34-EDC does not change the intensity of punctate and vacuolar Envy-Vps34 localized to the vacuole. *vps34Δ* cells were transformed with pRS416-Envy-Vps34 or pRS416-Envy-Vps34-EDC. After labeling with FM 4-64, cells were chased at 24°C for 3 h before imaging. DIC, differential interference contrast. Scale bar = 5 μm. The Envy-Vps34 signal that overlaps FM 4-64 was divided by the number of cells quantified. Quantification of at least 100 cells per n, n=3. The average of the wild-type samples was normalized to 1. Error bars indicate standard deviation. Unpaired t-test. ns=p>.05.

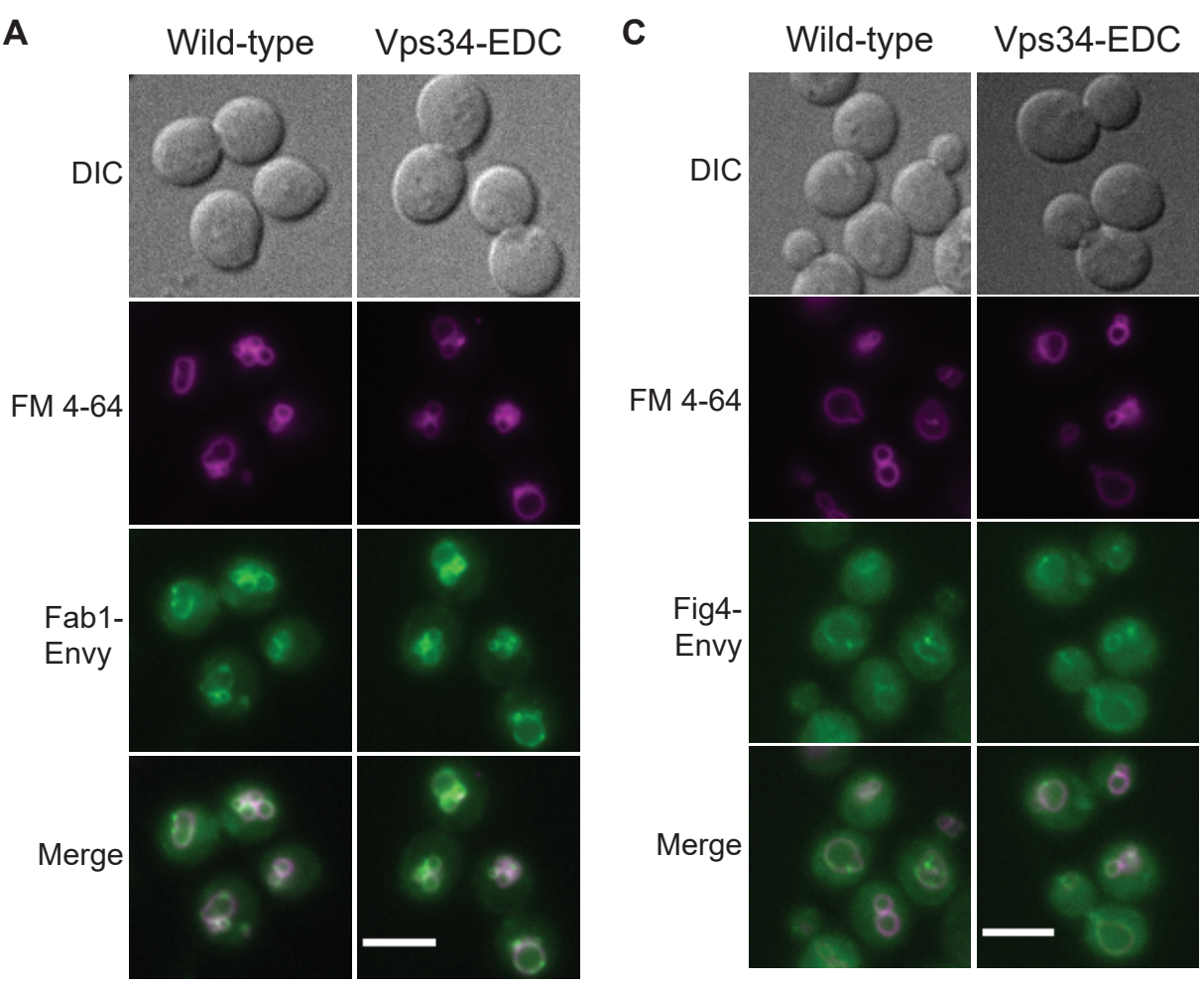

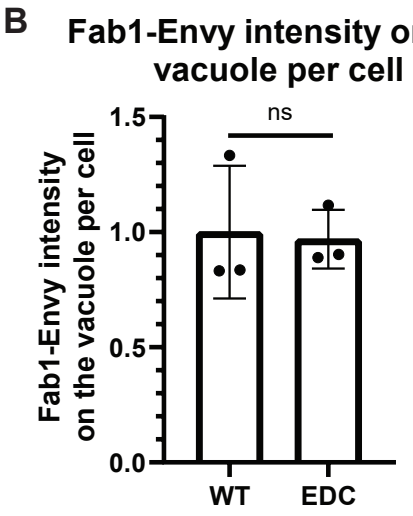

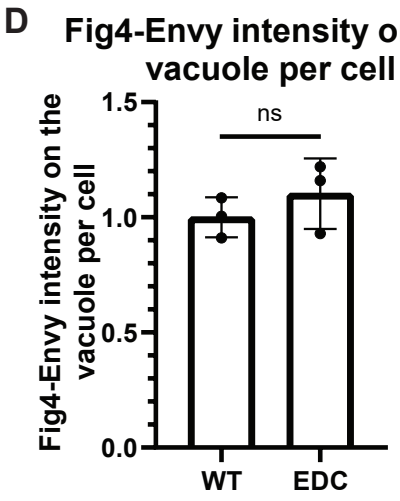

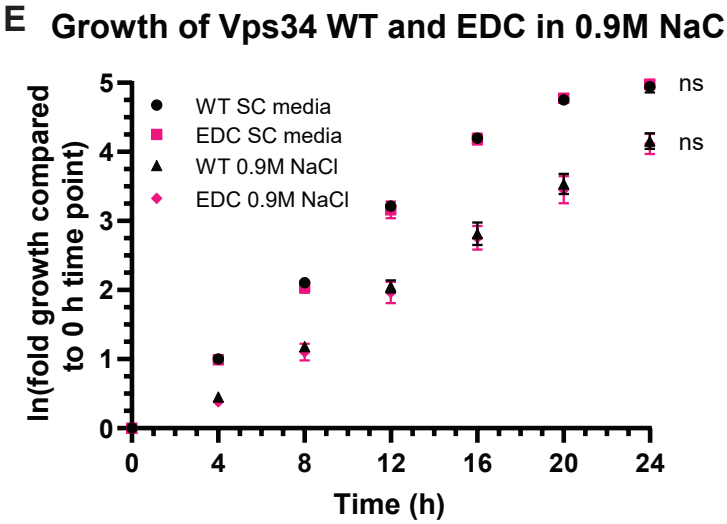

Figure S4. Hyperactive Vps34-EDC does not affect the localization of some members of the $PI(3,5)P_2$ kinase complex

Figure S4. Hyperactive Vps34-EDC does not affect the localization of some members of the PI(3,5)P_2 kinase complex. (A and B) Hyperactive Vps34-EDC does not change the localization of Fab1-Envy to the vacuole. *vps34Δ* cells were transformed with pRS416-Fab1-Envy and pRS413-Vps34 or pRS413-Vps34-EDC. After labeling with FM 4-64, cells were chased at 24°C for 3 h before imaging. DIC, differential interference contrast. Scale bar = 5 μm. The Fab1-Envy signal that overlaps FM 4-64 was divided by the number of cells quantified. Quantification of at least 100 cells per n, n=3. The average of the wild-type samples was normalized to 1. Error bars indicate standard deviation. Unpaired t-test. ns=p>.05. (C and D) Hyperactive Vps34-EDC does not change the localization of Fig4-Envy to the vacuole. *vps34Δ* cells were transformed with pRS413-Fig4-Envy and pRS416-Vps34 or pRS416-Vps34-EDC. After labeling with FM 4-64, cells were chased at 24°C for 3 h before imaging. DIC, differential interference contrast. Scale bar = 5 μm. The Fig4-Envy signal that overlaps FM 4-64 was divided by the number of cells quantified. Quantification of at least 100 cells per n, n=3. The average of the wild-type samples was normalized to 1. Error bars indicate standard deviation. Unpaired t-test. ns=p>.05. (E) Hyperactive Vps34-EDC does not affect the growth of yeast cells following hyperosmotic shock. *vps34Δ* cells were transformed with pRS416-Vps34 or pRS416-Vps34-EDC. Cells were grown to mid-log phase in SC media and then diluted to equal concentrations. An equal volume of SC media or SC media with 1.8 M NaCl was added to the culture to begin the time-course. ODs were measured immediately following the addition of SC media or SC media with 1.8 M NaCl and then every 4 h for 24 h. The time zero OD measurement for each sample was normalized to 1. A natural logarithmic transformation was applied to the normalized ODs so that exponential growth is represented linearly. n=4. Error bars indicate standard deviation. Unpaired t-test between WT and EDC at each time point. ns=p>.05.

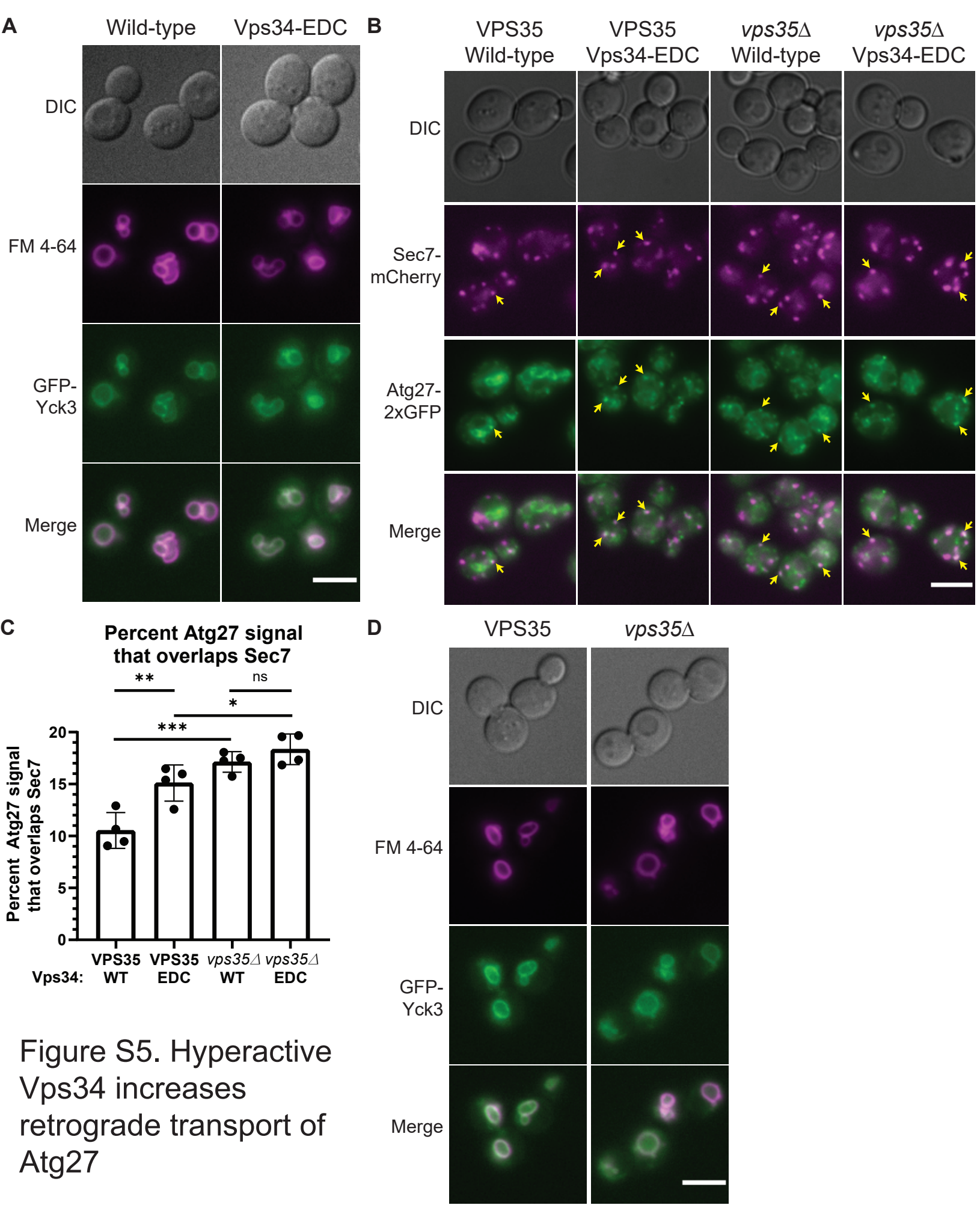

Figure S5. Hyperactive Vps34 increases retrograde transport of Atg27

Figure S5. Hyperactive Vps34 increases retrograde transport of Atg27. (A) Hyperactive Vps34-EDC does not change the localization of the GFP-Yck3 kinase, an AP-3 client protein localized to the vacuole membrane. *vps34Δ* cells were co-transformed with pRS413-Vps34 or pRS413-Vps34-EDC and pRS416-GFP-Yck3. After labeling with FM 4-64, cells were chased at 24°C for 3 h before imaging. DIC, differential interference contrast. Scale bar = 5 μm. At least 40 cells per n, n=3. (B and C) Atg27-2xGFP partially colocalizes with the trans-Golgi (Sec7-mCherry). This colocalization increases in the presence of hyperactive Vps34-EDC. In the absence of *VPS35*, Atg27-2xGFP colocalization with the trans-Golgi is unchanged between wild-type and Vps34-EDC. *vps34Δ* or *vps34Δ vps35Δ* cells with Atg27-2xGFP and Sec7-mCherry integrated at the endogenous loci were transformed with pRS416-Vps34 or pRS416-Vps34-EDC. DIC, differential interference contrast. Scale bar = 5 μm. Examples of Atg27-2xGFP puncta that colocalize with Sec7-mCherry are indicated by yellow arrows. The Atg27-2xGFP signal that overlaps Sec7-mCherry was divided by total Atg27-2xGFP signal. Quantification of at least 40 cells per n, n=4. Error bars indicate standard deviation. Unpaired t-test. ns=p>.05, *=p<.05, **=p<.01, ***=p<.001. (D) Deletion of *VPS35* does not change the localization of the GFP-Yck3 kinase, an AP-3 client protein localized to the vacuole membrane. Wild-type or *vps35Δ* cells were transformed with pRS416-GFP-Yck3. After labeling with FM 4-64, cells were chased at 24°C for 3 h before imaging. DIC, differential interference contrast. Scale bar = 5 μm. At least 40 cells per n, n=4.

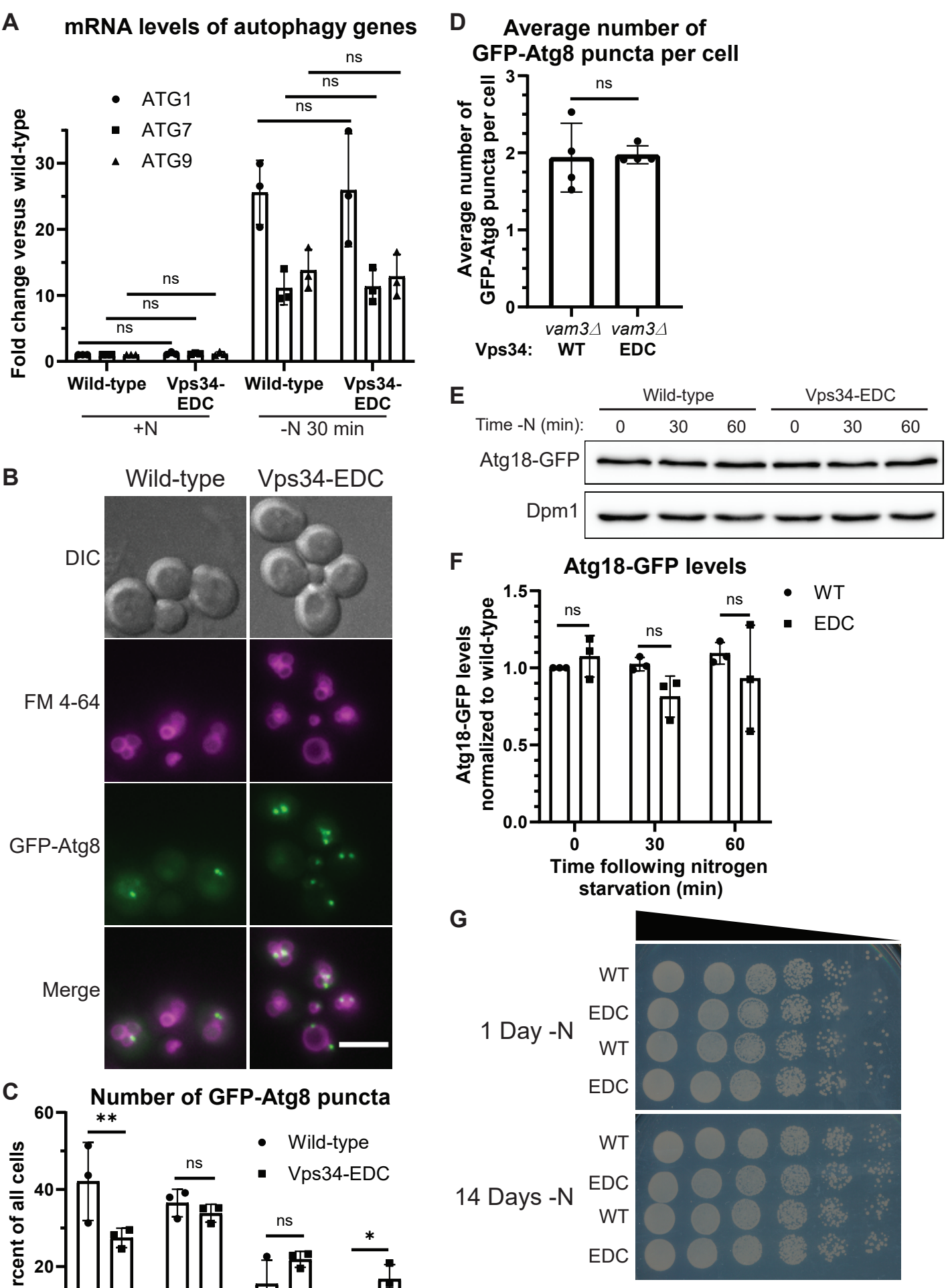

Figure S6. Hyperactive Vps34 inhibits a late step in autophagy

Figure S6. Hyperactive Vps34 inhibits a late step in autophagy. (A) mRNA levels of *ATG1*, *ATG7*, and *ATG9* are unchanged between Vps34-EDC and wild-type, suggesting that Vps34-EDC does not affect the transcription of select autophagy genes. *vps34Δ* cells were transformed with pRS416-Vps34 or pRS416-Vps34-EDC. *ATG1*, *ATG7*, and *ATG9* mRNA transcript levels were measured by qRT-PCR in nitrogen rich conditions and following 30 min of nitrogen starvation. mRNA levels were normalized to wild-type in nitrogen rich conditions. n=3. Error bars indicate standard deviation. Unpaired t-test. ns=p>.05. (B and C) Hyperactive Vps34-EDC results in an increase in the number of GFP-Atg8 puncta in cells following 30 min of nitrogen starvation. *vps34Δ* cells were co-transformed with pRS414-GFP-Atg8 and pRS416-Vps34 or pRS416-Vps34-EDC. After labeling with FM 4-64, cells were chased at 24°C for 3 h before 9 z-slices that were 0.2 μm apart were imaged. Maximum intensity projection. DIC, differential interference contrast. Scale bar = 5 μm. GFP-Atg8 puncta were counted by a scorer who was blinded to the genotype of the cells being quantified. Quantification of at least 100 cells per n, n=3. Error bars indicate standard deviation. Two-way ANOVA and Dunnett's post-hoc test. ns=p>.05, *=p<.05, **=p<.01. (D) Hyperactive Vps34-EDC does not cause an increase in the number of GFP-Atg8 puncta in *vam3Δ* cells after 1 h of nitrogen starvation. This experiment is an alternative quantification of the experiment performed in Figure 5D and E. *vps34Δ vam3Δ* cells with Atg18-RFP integrated at the endogenous locus were transformed with pRS413-GFP-Atg8 and pRS416-Vps34 or pRS416-Vps34-EDC. GFP-Atg8 puncta were counted by a scorer who was blinded to the genotype of the cells being quantified. Cells without visible Atg18-RFP were excluded from quantification. Quantification of 100 cells per n, n=4. Error bars indicate standard deviation. Unpaired t-test. ns=p>.05. (E and F) Vps34-EDC does not change Atg18-GFP protein levels at basal conditions or during nitrogen starvation. *vps34Δ* cells were co-transformed with pRS413-Vps34 or pRS413-Vps34-EDC and pRS416-Atg18-GFP. Atg18-GFP protein levels were analyzed via western blot using anti-GFP antibody. Atg18-GFP levels were normalized to Dpm1. Levels were then normalized to wild-type at basal conditions. Representative of n=3. Error bars indicate standard deviation. Unpaired t-test. ns=p>.05. (G) Hyperactive Vps34-EDC does not affect the survival of yeast cells during long-term nitrogen starvation. *vps34Δ* cells were transformed with pRS416-Vps34 or pRS416-Vps34-EDC and grown to mid-log phase in SC media. Equal numbers of cells were collected and rinsed twice in nitrogen-starvation media before resuspending in nitrogen-starvation media. Following 1 day and 14 days of nitrogen starvation, equal volumes of culture were serially diluted 1:5 and spotted on SC plates. Plates were imaged following 3 days of yeast growth. 2 representative samples of n=4.

Table S1. **Yeast strains used in this study**

Strain	Genotype	Source	Figure used
LWY13700	*MATa, leu2,3-112, ura3-52, his3-Δ200, trp1-Δ901, lys2-801, suc2-Δ9, vps34Δ::KAN*	This study	1D-F, 3A-D, 4A-F, 6A-C, S1D+E, S2A and C+D, S3A-D, S4A-E, S5A, S6A-C and E-G
LWY19264	*MATalpha, leu2,3-112, ura3-52, his3-Δ200, trp1-Δ901, lys2-801, suc2-Δ9, vps34Δ::KAN, Atg27-2xGFP::HIS3*	This study	2A-C
LWY19252	*MATalpha, leu2,3-112, ura3-52, his3-Δ200, trp1-Δ901, lys2-801, suc2-Δ9, vps34Δ::KAN, Atg27-2xGFP::HIS3, snx4Δ::HYG*	This study	2A-C
LWY19306	*MATa, leu2,3-112, ura3-52, his3-Δ200, trp1-Δ901, lys2-801, suc2-Δ9, vps34Δ::KAN, Atg27-2xGFP::HIS3, Sec7-mCherry::HYG*	This study	2D+E
LWY19358	*MATa, leu2,3-112, ura3-52, his3-Δ200, trp1-Δ901, lys2-801, suc2-Δ9, vps34Δ::KAN, Atg27-2xGFP::HIS3, Vps8-mCherry::HYG*	This study	2F+G
LWY19146	*MATalpha, leu2,3-112, ura3-52, his3-Δ200, trp1-Δ901, lys2-801, suc2-Δ9, vps34Δ::HYG*	This study	5A-C
LWY19144	*MATa, leu2,3-112, ura3-52, his3-Δ200, trp1-Δ901, lys2-801, suc2-Δ9, vps34Δ::HYG, ymr1Δ::HIS3*	This study	5A-C
LWY19450	*MATa, leu2,3-112, ura3-52, his3-Δ200, trp1-Δ901, lys2-801, suc2-Δ9, vps34Δ::HYG, Atg18-RFP::TRP1*	This study	5D+E
LWY19453	*MATa, leu2,3-112, ura3-52, his3-Δ200, trp1-Δ901, lys2-801, suc2-Δ9, vps34Δ::HYG, Atg18-RFP::TRP1, vam3Δ::NAT*	This study	5D+E, S6D
LWY7235	*MATa, leu2,3-112, ura3-52, his3-Δ200, trp1-Δ901, lys2-801, suc2-Δ9*	(Bonangelino *et al.*, 1997)	S1A+B, S5D
LWY19518	*MATa, leu2,3-112, ura3-52, his3-Δ200, trp1-Δ901, lys2-801, suc2-Δ9, vps34Δ::KAN, Atg27-2xGFP::HIS3, Sec7-mCherry::HYG*	This study	S5B+C
LWY19521	*MATalpha, leu2,3-112, ura3-52, his3-Δ200, trp1-Δ901, lys2-801, suc2-Δ9, vps34Δ::KAN, Atg27-2xGFP::HIS3, Sec7-mCherry::HYG, vps35Δ::NAT*	This study	S5B+C
LWY19503	*MATalpha, leu2,3-112, ura3-52, his3-Δ200, trp1-Δ901, lys2-801, suc2-Δ9, vps35Δ::NAT*	This study	S5D

Table S2. **Yeast plasmids used in this study**

Plasmid	Description	Source	Figure used
pRS416-Vps34	CEN, URA3	This study	1D-F, 2A-G, 3A-D, 4A-F, 5A-E, 6A-C, S1D+E, S2A and C+D, S4C-E, S5B+C, S6A-D and G
pRS416-Vps34-R283E A287D	CEN, URA3	This study	1D-F, S1E, S2D
pRS416-Vps34-Y501C	CEN, URA3	This study	1D-F, S2C+D
pRS416-Vps34-EDC	CEN, URA3	This study	1D-F, 2A-G, 3A-D, 4A-F, 5A-E, 6A-C, S2D, S4C-E, S5B+C, S6A-D and G
pRS414-Ypq1-GFP	CEN, TRP1	Subcloned from (Li *et al.*, 2015)	3A+B
pRS414-Mup1-GFP	CEN, TRP1	Subcloned from (Lin *et al.*, 2008)	3C+D
pRS414-GFP-Atg8	CEN, URA3	(Abeliovich *et al.*, 2003)	4E+F, S6B+C
pRS414-pCup1-GFP-Atg8	CEN, TRP1	(Abeliovich *et al.*, 2003)	5A+B
pRS413-GFP-Atg8	CEN, HIS3	Subcloned from (Abeliovich *et al.*, 2003)	5D+E, S6D
pRS426-GFP-Vps34	2µ, URA3	This study	S1A+B
pRS425-Vps15-13xMyc	2µ, LEU2	This study	S1A+B
pRS416-Vps34-D275K	CEN, URA3	This study	S1D
pRS416-Vps34-R283E	CEN, URA3	This study	S1D+E
pRS416-Vps34-A287D	CEN, URA3	This study	S1D+E
pRS416-Vps34-N292D	CEN, URA3	This study	S1D
pRS416-Vps34-H322A	CEN, URA3	This study	S1D
pRS416-Vps34-E323D	CEN, URA3	This study	S1D
pRS416-Vps34-F761Y	CEN, URA3	This study	S1D
pRS416-Vps34-I863D	CEN, URA3	This study	S1D
pRS416-Vps34- D275K R283E A287D N292D	CEN, URA3	This study	S1E
pRS416-Vps34-D275K R283E A287D N292D H322A	CEN, URA3	This study	S1E
pRS416-Vps34-K759D	CEN, URA3	This study	S2A
pRS416-Vps34-E505G	CEN, URA3	This study	S2C
pRS416-Vps34-S506P	CEN, URA3	This study	S2C
pRS416-Vps34-D628V	CEN, URA3	This study	S2C
pRS416-Vps34-M642V	CEN, URA3	This study	S2C
pRS416-5xHA-Vps34	CEN, URA3	This study	S3A+B
pRS416-5xHA-Vps34-EDC	CEN, URA3	This study	S3A+B
pRS416-Envy-Vps34	CEN, URA3	This study	S3C+D

pRS416-Envy-Vps34-EDC	CEN, URA3	This study	S3C+D
pRS413-Vps34	CEN, HIS3	This study	S4A+B, S5A, S6E+F
pRS413-Vps34-EDC	CEN, HIS3	This study	S4A+B, S5A, S6E+F
pRS416-Fab1-Envy	CEN, URA3	This study	S4A+B
pRS413-Fig4-Envy	CEN, HIS3	This study	S4C+D
pRS416-GFP-Yck3	CEN, URA3	This study	S5A+D
pRS416-Atg18-GFP	CEN, URA3	(Rieter *et al.*, 2013)	S6E+F